J. Indian Chem. Soc.,
Vol. 96, December 2019, pp. 1483-1492

Graph theoretical study of stabilization of some IPR fullerenes by cage closure

Bankim Chandra Ghosh

Department of Chemistry, Durgapur Government College, J. N. Avenue, Durgapur-713 214, West Bengal, India

E-mail: bankimghosh@yahoo.co.in

Manuscript received online 09 November 2019, accepted 18 November 2019

Fullerene structures can be built up step by step by adding C_2-fragments to pentagons and hexagons of sp^2-carbon atoms systematically; if in this building process fusion of pentagons are avoided and the Euler formula is obeyed, structures of carbon cages corresponding to the IPR fullerenes are obtained. Graph theoretical method involving 5- and 6-fold rotational symmetry can be used to obtain the π-MO energies of the sub-structures and also of the complete cage structure. This has been done in the present work and it has been shown that the total π-electron energy per atom gradually decreases as the sub-structures grow with addition of C_2-fragments and in the last step when the cage closure is complete, the stabilization is very much appreciable. The method has been shown with the IPR fullerenes C_{60}, C_{70}, C_{72} and C_{84}.

Keywords: Graph theory, fullerene, reduced graph, rotational symmetry.

1. Introduction

Fullerenes with all the 12 pentagons isolated by intervening hexagons, called IPR fullerenes, are known to be exceptionally stable[1] compared to other fullerenes of the same number of carbon atoms but with fused pentagons. Such stability is obviously related to bond angle strains which, in turn, results primarily from σ-electron repulsions. However, these carbon clusters consist of all near-sp^2 hybridized C atoms and the interactions of the π-electrons contributing to their stability through π-MO formation are also of considerable importance. Theoretically rigorous methods like all electron Green's function calculations and density functional theory are currently being applied for fullerenes, nanotubes and graphenes[2–6].

Graph theoretical methods are known[7–9] to yield the relative stabilities of π-conjugated systems in a simpler way and the results are known to be reliably in line with those predicted by the sophisticated methods. Graphs representing the structures of fullerenes can be built up step by step[10–12] by adding C_2-fragments to pentagons and hexagons of sp^2-C atoms; in this building process fusion of pentagons is avoided and the Euler formula is followed to obtain closed carbon cages. Graph theoretical method involving 5- and 6-fold rotational symmetry can be used to obtain the π-MO energies of the sub-structures and also of the complete fullerene. In the present work, the total π-electron energy per atom has been calculated graph theoretically for the building units (sub-structures) and also of the whole IPR fullerene to investigate how the contribution of π-electrons to stability gradually changes in the series of sub-structures and the whole structure; this has been done with the IPR fullerenes C_{60}, C_{70}, C_{72} and C_{84}.

2. Step by step construction of the fullerene graphs from pentagons and hexagons by adding single vertices and K_2 sub-graphs

Starting from a pentagon, (A), a C_{10} structure (B), which is a fullerene sub-structure, can be obtained by adding one vertex to each vertex of the pentagon. In each '*bay*' region thus produced a K_2 sub-graph is placed and the pendent vertices of C_{10} (B) are joined to the vertices of K_2 to get a hexagon; the original pentagon (A) is now surrounded by five fused hexagons giving a C_{20} sub-structure (C) of a fullerene. To each '*vee*' region of C_{20}, a K_2 sub-graph is added and thus the sub-structure (C) is surrounded by five isolated pentagons, thereby yielding C_{30}, (D). In this way, progressively, one obtains the C_{50} sub-structure, (F) (Fig. 1). This is common to both C_{60} and C_{70}. Starting from (F) the construction of fullerene structures (H) for C_{60} and (K) for C_{70} can be obtained (Fig. 2). Construction of the series (A′),(B′),...,(K′) of sub-structures and structures for C_{72} and C_{84} starting from a hexagon is done by a similar procedure (Figs. 3 and 4). Details of this procedure can be found in references[10,11]. It

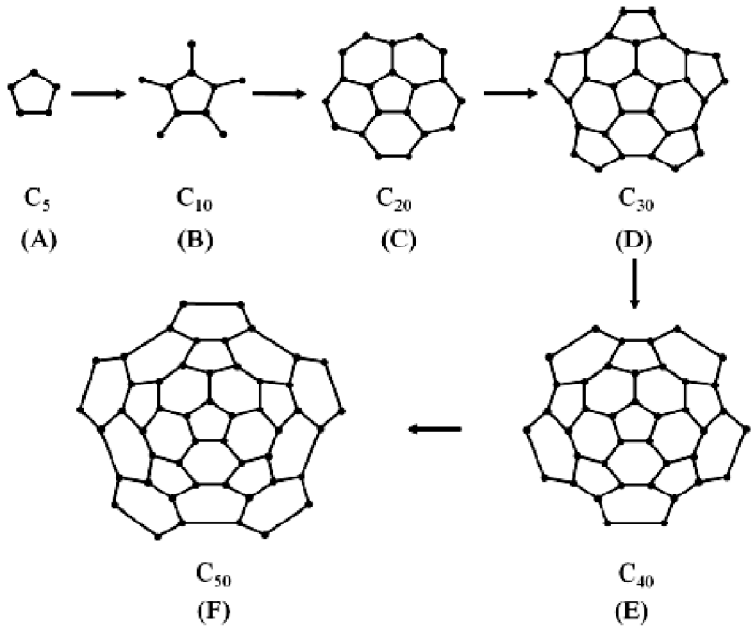

Fig. 1. Construction of sub-structures of [60]- and [70]-fullerenes maintaining 5-fold symmetry.

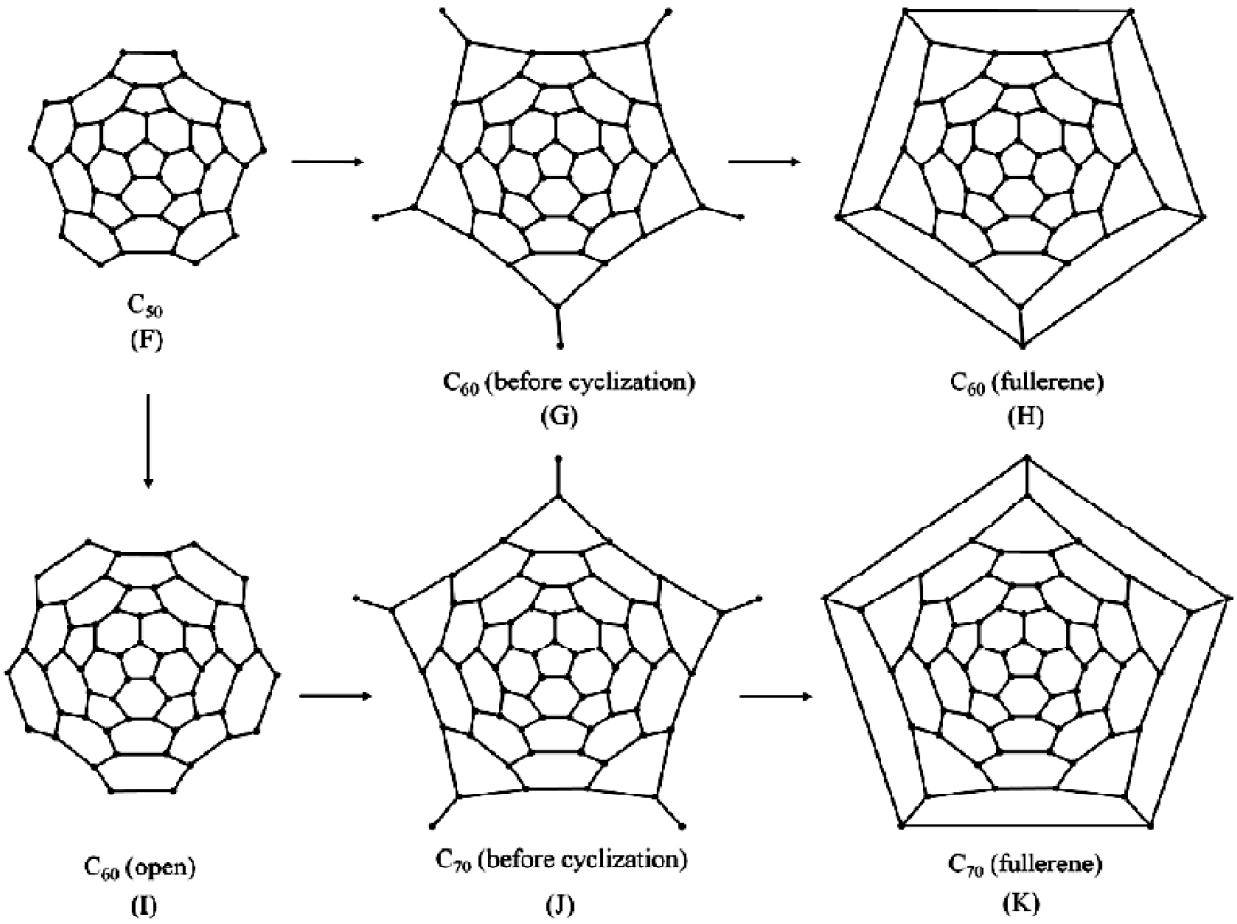

Fig. 2. Cage closure for [60]- and [70]-fullerenes starting from the C_{50} sub-structure and maintaining 5-fold symmetry.

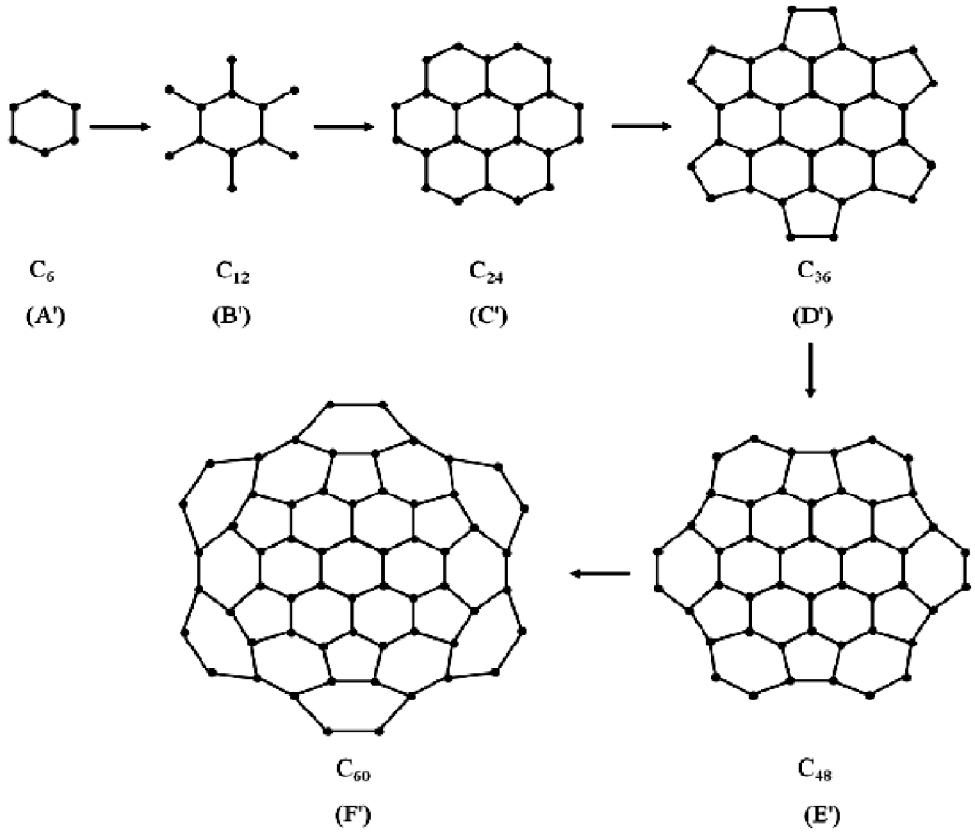

Fig. 3. Construction of sub-structures of [72]- and [84]-fullerenes maintaining 6-fold symmetry.

is to be noted that 5-fold rotational symmetry is maintained in the series (A),(B),···,(K); similarly the series (A′), (B′),···,(K′) maintains 6-fold rotational symmetry.

3. Construction of reduced graphs for the structures and sub-structures by utilizing rotational symmetry

Following the method developed by Davidson[13] and Shen[14] a graph with N vertices having r-fold rotational symmetry ($r \geq 2$) can be classified into orbits such that a r-fold rotation transforms any vertex of a particular orbit into another vertex of the same orbit but vertices of different orbits are not interconvertible by that rotation. Scheme for labeling of the vertices for utilizing r-fold rotation is as follows:

Orbit No. 1:

Vertex labels: 1,(1+ N/r),(1+ $2N/r$),(1+ $3N/r$),.....,r-th term

Orbit No. 2:

Vertex labels: 2,(2 + N/r),(2 + $2N/r$),(2 + $3N/r$),.....,r-th term

……

Orbit No. r:

Vertex labels: r,(r + N/r),(r + $2N/r$),(r + $3N/r$),.....,r-th term

This labeling scheme is illustrated for C_{60} fullerene (H) in Fig. 5. Such a labeling scheme makes the adjacency matrix of any graph with r-fold rotational symmetry circulantly partitioned:

$$\begin{bmatrix} \mathbf{A}_1 & \mathbf{A}_2 & \cdots & \cdots & \mathbf{A}_{r-1} & \mathbf{A}_r \\ \mathbf{A}_r & \mathbf{A}_1 & \mathbf{A}_2 & \cdots & \cdots & \mathbf{A}_{r-1} \\ \mathbf{A}_{r-1} & \mathbf{A}_r & \mathbf{A}_1 & \cdots & \cdots & \mathbf{A}_{r-2} \\ \mathbf{A}_{r-2} & \mathbf{A}_{r-1} & \mathbf{A}_r & \cdots & \cdots & \mathbf{A}_{r-3} \\ \cdots & \cdots & \cdots & \cdots & \cdots & \cdots \\ \mathbf{A}_2 & \mathbf{A}_3 & \cdots & \cdots & \mathbf{A}_r & \mathbf{A}_1 \end{bmatrix}$$

For example with the coranulene sub-structure (C_{20} system, (C) of Fig. 1) the following matrices will appear as the component blocks of the whole adjacency matrix:

$$\mathbf{A}_1 = \begin{bmatrix} 0 & 1 & 0 & 0 \\ 1 & 0 & 1 & 0 \\ 0 & 1 & 0 & 1 \\ 0 & 0 & 1 & 0 \end{bmatrix}, \quad \mathbf{A}_2 = \begin{bmatrix} 1 & 0 & 0 & 0 \\ 0 & 0 & 0 & 0 \\ 0 & 0 & 0 & 0 \\ 0 & 1 & 0 & 0 \end{bmatrix},$$

$$\mathbf{A}_3 = \begin{bmatrix} 0 & 0 & 0 & 0 \\ 0 & 0 & 0 & 0 \\ 0 & 0 & 0 & 0 \\ 0 & 0 & 0 & 0 \end{bmatrix} = \mathbf{A}_4 \text{ and } \mathbf{A}_5 = \begin{bmatrix} 0 & 1 & 0 & 0 \\ 0 & 0 & 0 & 1 \\ 0 & 0 & 0 & 0 \\ 0 & 0 & 0 & 0 \end{bmatrix}$$

According to the Davidson-Shen algorithm[13,14] circulantly partitioned matrices resulting from *r*-fold rotational symmetry transform into block diagonal matrices; there will be *r* number of blocks of dimension $\left(\frac{N}{r} \times \frac{N}{r}\right)$ and each block matrix is represented as

$$\mathbf{B}_{j+1} = \sum_{r=0}^{(r-1)} \mathbf{A}_{r+1} \varepsilon^{r \times j}, \; j = 0 \text{ to } (r-1),$$

$$\text{where }, \; \varepsilon = e^{\frac{2\pi i}{r}}, i = \sqrt{-1} \tag{1}$$

4. Construction of the reduced graphs for the structures and sub-structures

Any block $\mathbf{B}_{j+1}$ may be considered as the adjacency matrix of a graph which may be constructed such that there are $\frac{N}{r}$ vertices, the non-zero diagonal elements of $\mathbf{B}_{j+1}$ are the self-loop weights of the vertices and the non-zero off-diagonal elements are the edge-weights; zero diagonal elements

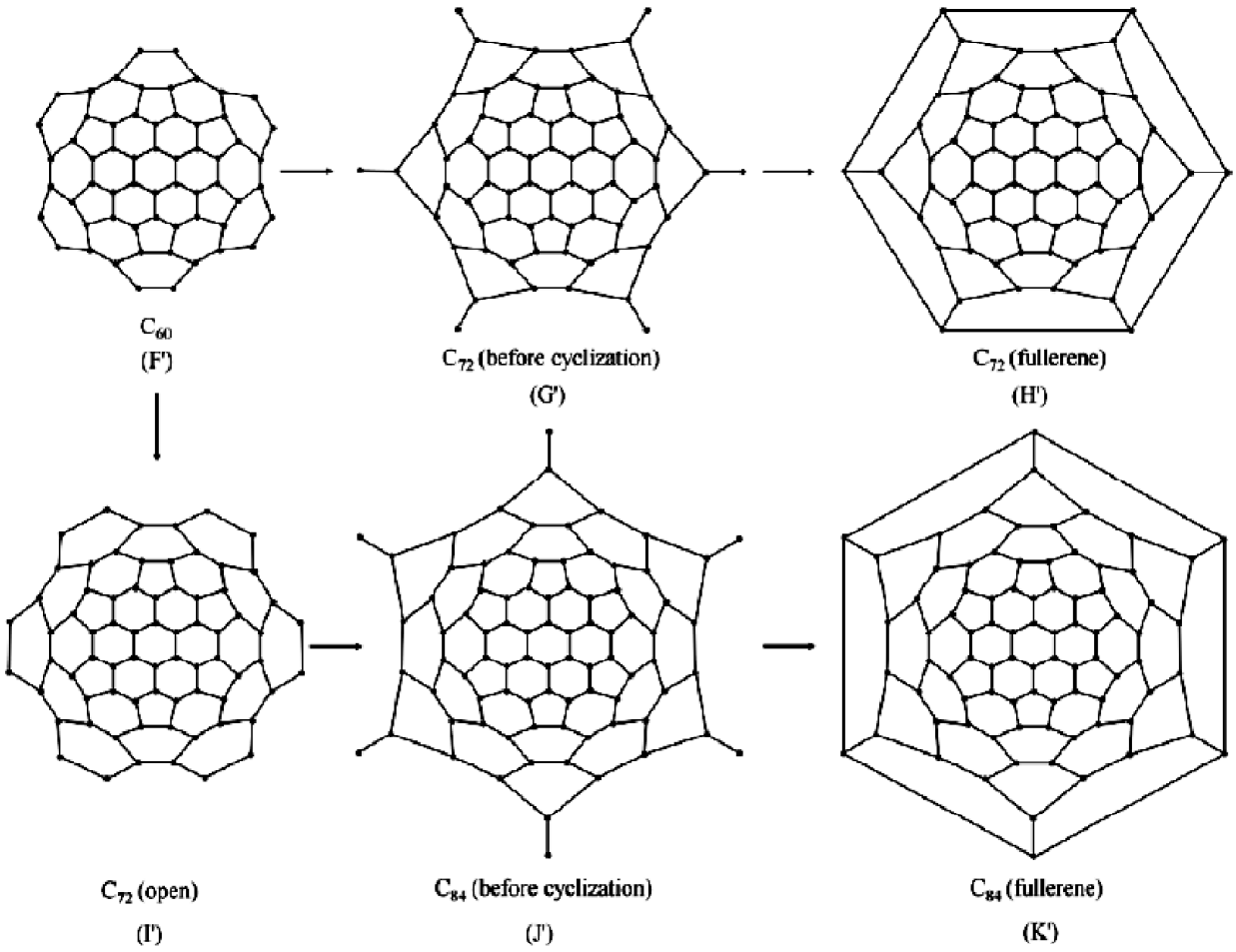

Fig. 4. Cage closure for [72]- and [84]-fullerenes starting from the C_{60} sub-structure and maintaining 6-fold symmetry.

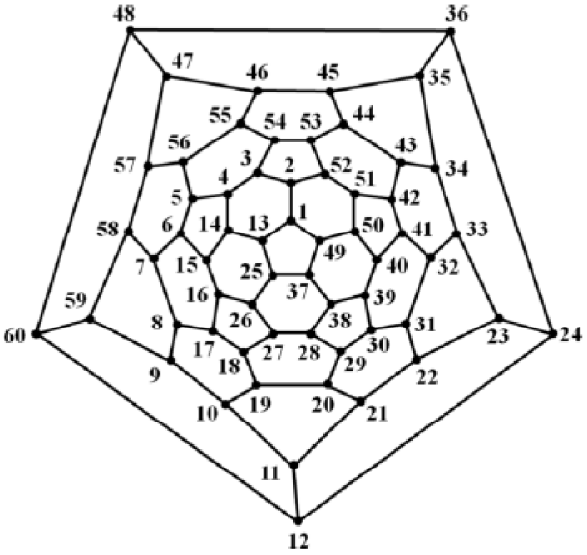

Fig. 5. Vertex labeling of C_{60} fullerene using 5-fold symmetry.

correspond to unweighted vertices and whenever an off-diagonal element) (p,q) is zero, the vertices p and q are disconnected. A graph thus obtained is a reduced graph representing a block $\mathbf{B}_{j+1}$. A single reduced graph represents all the blocks, $\mathbf{B}_{j+1}$, j = 0 to $(r-1)$ with the permitted values of $\varepsilon = e^{\frac{2\pi i}{r}}$. In constructing the reduced graph, the following identities related to the r-th roots of unity are utilized.

In case of 5-fold symmetry,

$$\varepsilon^m + (\varepsilon^m)^* = 2, -\frac{1}{2}+\frac{\sqrt{5}}{2}, -\frac{1}{2}-\frac{\sqrt{5}}{2}, -\frac{1}{2}+\frac{\sqrt{5}}{2}, -\frac{1}{2}-\frac{\sqrt{5}}{2}$$

for m = 0, 1, 2, 3 and 4 respectively.

In case of 6-fold symmetry,

$\varepsilon^m + (\varepsilon^m)^*$ = 2,1,–1,–2,–1,1 for m = 0, 1, 2, 3, 4 and 5 respectively.

In this way the reduced graphs for all the structures and sub-structures of the fullerenes under consideration have been drawn and are shown in Fig. 6 where $a = \varepsilon^m$. Two points are to be mentioned here: (i) almost all the reduced graphs are directed graphs and (ii) the structures and sub-structures of the fullerene pair (C_{60}, C_{72}) have similar series of reduced graphs; same is the case with the pair (C_{70}, C_{84}). However, since ε is different for 5- and 6-fold rotational symmetry, the vertex- and edge-weight are different in the reduced graphs which appear to be similar.

As an illustration we show here the common form of the block matrices for the IPR fullerenes C_{60} and C_{72}:

$$\begin{bmatrix}
(a+a^*) & 1 & 0 & 0 & 0 & 0 & 0 & 0 & 0 & 0 & 0 \\
1 & 0 & 1 & a^* & 0 & 0 & 0 & 0 & 0 & 0 & 0 \\
0 & 1 & 0 & 1 & 0 & a^* & 0 & 0 & 0 & 0 & 0 \\
0 & a & 1 & 0 & 1 & 0 & 0 & 0 & 0 & 0 & 0 \\
0 & 0 & 0 & 1 & 0 & 1 & 0 & a^* & 0 & 0 & 0 \\
0 & 0 & a & 0 & 1 & 0 & 1 & 0 & 0 & 0 & 0 \\
0 & 0 & 0 & 0 & 0 & 1 & 0 & 1 & 0 & a^* & 0 \\
0 & 0 & 0 & 0 & a & 0 & 1 & 0 & 1 & 0 & 0 \\
0 & 0 & 0 & 0 & 0 & 0 & 0 & 1 & 0 & 1 & a^* \\
0 & 0 & 0 & 0 & 0 & 0 & a & 0 & 1 & 0 & 1 \\
0 & 0 & 0 & 0 & 0 & 0 & 0 & 0 & a & 1 & 0 \\
0 & 0 & 0 & 0 & 0 & 0 & 0 & 0 & 0 & 1 & (a+a^*)
\end{bmatrix}$$

These blocks are represented by the reduced graph (H, H′) in Fig. 6.

5. Characteristic polynomials and eigenvalues of the structures and sub-structures of the fullerenes

The characteristic polynomials of the reduced graphs in terms of b (= $a + a^*$) for the structures and sub-structures of the systems C_{60}, C_{70}, C_{72} and C_{84} are given in Table 1. These polynomials were constructed by the usual Laplacian expansion of the determinant $|x\mathbf{I} - \mathbf{B}_{j+1}|$ where $\mathbf{I}$ is the unit matrix of the size of $\mathbf{B}_{j+1}$. The graph eigenvalues are the zeros of the polynomials obtained by using the permitted values of b. Since one value of b is 2 for both 5- and 6-fold symmetries, the corresponding eigenvalues for all the systems under study are collected in Table 2. With $b = \left(-\frac{1}{2} \pm \frac{\sqrt{5}}{2}\right)$ for 5-fold symmetry the eigenvalues are doubly degenerate and are given in Table 3. Eigenvalues resulting from b = ±1, –2 for 6-fold symmetry are collected in Table 4 for all the structures and sub-structures under study; in this case the eigenvalues are doubly degenerate for b = ±1 and non-degenerate for b = –2.

6. Variation of total π-electron energy per atom in the series of structures and sub-structures

It may be noted that the sub-structures (A to F) of the fullerenes C_{60} and C_{70} are the same up to the C_{50} unit. From this the open C_{60} sub-structure (I) can be obtained by adding five K_2 subgraphs vertically in the '*bay*' regions and then the C_{60} fullerene cage (H) is completed by joining the pendent vertices. Similarly, the open C_{70} sub-structure (J) is obtained from (F) by adding five K_2 subgraphs horizontally

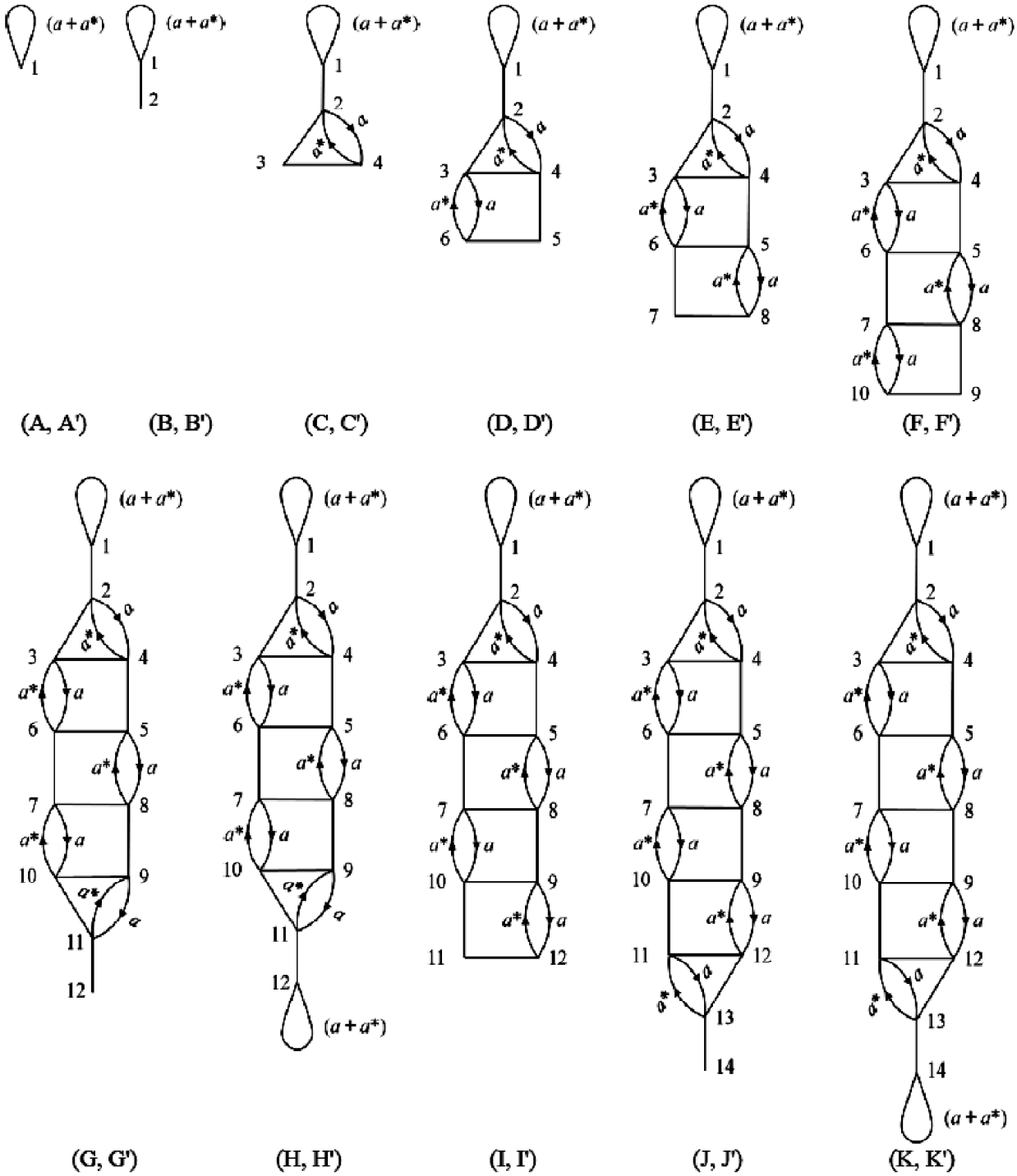

Fig. 6. Reduced graphs of the structures shown in Figs. 1-4 on application of 5- and 6-fold rotational symmetries.

Table 1. Characteristics polynomials of the reduced graphs shown in Fig. 6 [$b = a + a^*$]

Reduced graph	Characteristics polynomial
(A, A′)	$x - b$
(B, B′)	$x^2 - bx - 1$
(C, C′)	$x^4 - bx^3 - 4x^2 + 2bx + (b^2 + 1)$
(D, D′)	$x^6 - bx^5 - 7x^4 + 5bx^3 + (b^2 - b + 10)x^2 + (b^2 - 5b - 2)x - (b^2 - 3b + 2)$
(E, E′)	$x^8 - bx^7 - 10x^6 + 8bx^5 + (b^2 - 2b + 28)x^4 + (2b^2 - 17b - 2)x^3 - (4b^2 - 8b + 24)x^2 - (3b^2 - 10b - 2)x - (b^3 - 3b^2 + 4b - 5)$
(F, F′)	$x^{10} - bx^9 - 13x^8 + 11bx^7 + (b^2 - 3b + 55)x^6 + (3b^2 - 38b - 2)x^5 - (7b^2 - 19b + 91)x^4 - (12b^2 - 50b - 8)x^3 - (2b^3 - 13b^2 + 30b - 57)x^2 - (b^3 - 10b^2 + 19b + 6)x + (2b^3 - 9b^2 + 12b - 9)$
(G, G′)	$x^{12} - bx^{11} - 16x^{10} + 13bx^9 + (2b^2 - 3b + 90)x^8 + (3b^2 - 57b - 4)x^7 - (18b^2 - 28b + 218)x^6 - (b^3 + 17b^2 - 105b - 28)x^5 - (4b^3 - 48b^2 + 75b - 226)x^4 + (3b^3 + 20b^2 - 75b - 44)x^3 + (9b^3 - 46b^2 + 65b - 82)x^2 + (b^4 - 3b^3 - 3b^2 + 9b + 12)x - (2b^3 - 9b^2 + 12b - 9)$
(H, H′)	$x^{12} - 2bx^{11} + (b^2 - 16)x^{10} + 28bx^9 - (10b^2 + 3b - 90)x^8 - (2b^3 - 6b^2 + 134b + 4)x^7 - (3b^3 - 28b^2 - 32b + 218)x^6 + (16b^3 - 42b^2 + 268b + 28)x^5 + (b^4 + 10b^3 - 19b^2 - 101b + 226)x^4 + (4b^4 - 38b^3 + 76b^2 - 210b - 44)x^3 - (3b^4 - b^3 + 21b^2 - 101b + 82)x^2 - (6b^4 - 30b^3 + 38b^2 - 34b - 12)x - (b^5 - 4b^4 + 9b^3 - 19b^2 + 18b - 9)$
(I, I′)	$x^{12} - bx^{11} - 16x^{10} + 14bx^9 + (b^2 - 4b + 91)x^8 + (4b^2 - 68b - 2)x^7 - (10b^2 - 36b + 230)x^6 - (27b^2 - 144b - 14)x^5 - (3b^3 - 33b^2 + 98b - 268)x^4 - (3b^3 - 50b^2 + 130b + 24)x^3 + (10b^3 - 46b^2 + 94b - 132)x^2 + (4b^3 - 27b^2 + 40b + 12)x - (b^4 - 7b^3 + 19b^2 - 28b + 20)$
(J, J′)	$x^{14} - bx^{13} - 19x^{12} + 16bx^{11} + (2b^2 - 4b + 135)x^{10} + (4b^2 - 93b - 4)x^9 - (24b^2 - 48b + 453)x^8 - (b^3 + 34b^2 - 250b - 40)x^7 - (6b^3 - 98b^2 + 190b - 752)x^6 + (4b^3 + 84b^2 - 318b - 116)x^5 + (29b^3 - 174b^2 + 298b - 588)x^4 + (2b^4 - 5b^3 - 66b^2 + 160b + 112)x^3 + (2b^4 - 34b^3 + 124b^2 - 176b + 184)x^2 - (2b^4 - 8b^3 - 4b^2 + 20b + 24)x - (b^4 - 7b^3 + 19b^2 - 28b + 20)$
(K, K′)	$x^{14} - 2bx^{13} + (b^2 - 19)x^{12} + 34bx^{11} - (13b^2 + 4b - 135)x^{10} - (2b^3 - 8b^2 + 212b + 4)x^9 - (4b^3 - 55b^2 - 52b + 453)x^8 + (22b^3 - 78b^2 + 612b + 40)x^7 + (b^4 + 24b^3 - 84b^2 - 228b + 752)x^6 + (6b^4 - 84b^3 + 238b^2 - 840b - 116)x^5 - (4b^4 + 28b^3 - 400b + 588)x^4 - (24b^4 - 136b^3 + 266b^2 - 480b - 112)x^3 - (2b^5 - 10b^4 + 18b^3 - 94b^2 + 264b - 184)x^2 - (2b^5 - 22b^4 + 70b^3 - 86b^2 + 72b + 24)x + (2b^5 - 13b^4 + 30b^3 - 39b^2 + 40b - 20)$

Table 2. Non-degenerate eigenvalues of the structures and sub-structures of the fullerene pairs (C_{60}, C_{72}) and (C_{70}, C_{84}) resulting from $b = 2$ in the characteristic polynomials

Pair of systems	Reduced graph	Non-degenerate eigenvalues
(C_5, C_6)	(A, A′)	2.00000
(C_{10}, C_{12})	(B, B′)	–0.41421, 2.41421
(C_{20}, C_{24})	(C, C′)	–1.21431, –1.00000, 1.53918, 2.67513
(C_{30}, C_{36})	(D, D′)	–2.00000, –1.34292, 0.00000, 0.52931, 2.00000, 2.81360
(C_{40}, C_{48})	(E, E′)	–2.41421, –1.37213, –1.00000, –0.08464, 0.41421, 1.33257, 2.24144, 2.88275
(C_{50}, C_{60})	(F, F′)	–2.61803, –1.61803, –1.37987, –0.41421, –0.38196, 0.61803, 0.70863, 1.75102, 2.41421, 2.92022
(C_{60}, C_{72})	(G, G′)	–2.61803, –1.6l803, –1.58889, –1.36110, –0.38197, –0.30620, 0.38196, 0.61803, 1.24312, 2.04927, 2.61803, 2.96380
(C_{60}, C_{72})	(H, H′)	–2.61803, –1.61803, –1.43828, –1.30278, –0.38197, –0.13856, 0.61803, 1.00000, 1.82025, 2.30278, 2.75660, 3.00000
(C_{60}, C_{72})	(I, I′)	–2.73205, –2.00000, –1.38207, –1.00000, –0.60118, 0.00000, 0.26006, 0.73205, 1.23602, 2.00000, 2.54456, 2.94241
(C_{70}, C_{84})	(J, J′)	–2.73205, –2.00000, –1.58328, –1.37654, –1.00000, –0.50516, 0.00000, 0.15863, 0.73205, 0.79533, 1.61133, 2.22362, 2.20458, 2.97148
(C_{70}, C_{84})	(K, K′)	–2.73205, –2.00000, –1.41421, –1.34292, –1.00000, –0.41421, 0.00000, 0.52931, 0.73205, 1.41421, 2.00000, 2.41421, 2.81360, 3.00000

Table 3. Doubly degenerate eigenvalues of the graphs shown in Figs. 1-4 resulting from

$$b = \left(-\frac{1}{2} \pm \frac{\sqrt{5}}{2} \right) \text{ for 5-fold symmetry}$$

System	Graph	Eigenvalues	
C_5	A	0.61803	–1.61803
C_{10}	B	–0.73764, 1.35567	–2.09529, 0.47726
C_{20}	C	–1.77748, –0.47725, 0.77748, 2.09529	–2.46672, –1.35567, 0.73764, 1.46673
C_{30}	D	–2.12438, –1.43566, –0.09433, 0.61803, 1.21902, 2.43535	–2.55715, –1.61803, –1.32015, 0.74989, 1.19940, 1.92800
C_{40}	E	–2.37719, –1.69925, –0.93665, –0.29946, 0.83145, 0.84804, 1.66186, 2.58923	–2.58314, –1.89257, –1.50774, –1.17137, 0.72141, 1.18097, 1.50224, 2.13218
C_{50}	F	–2.53314, –1.86770, –1.35421, –0.85935, –0.21577, 0.61803, 1.00000, 1.16095, 1.99749, 2.67173	–2.59271, –2.07497, –1.61802, –1.41664, –1.11747, 0.77241, 1.00000, 1.51435, 1.67201, 2.24302
C_{60}	G	–2.56316, –2.01848, –1.65193, –1.31075, –0.51421, –0.20078, 0.48229, 0.86998, 1.00000, 1.49509, 2.27943, 2.75055	–2.59693, –2.39203, –1.89568, –1.53604, –1.37857, –0.43209, 0.71631, 1.00000, 1.16173, 1.56868, 1.85554, 2.31183
C_{60}	H	–2.56156, –2.00000, –1.61803, –1.30278, –0.38197, –0.13856, 0.61803, 1.00000, 1.00000, 1.56154, 2.30278, 2.75660	–2.61803, –2.56156, –2.00000, –1.61803, –1.43828, –1.30278, 0.61803, 1.00000, 1.00000, 1.56154, 1.82025, 2.30278
C_{60}	I	–2.62790, –2.04567, –1.59776, –1.05910, –0.84574, –0.20870, 0.61803, 0.87055, 1.09426, 1.47895, 2.21958, 2.72153	–2.59682, –2.19023, –1.70213, –1.61804, –1.30218, –1.07187, 0.73282, 1.10179, 1.20638, 1.69796, 1.81414, 2.31016
C_{70}	J	–2.64601, –2.13440, –1.81334, –1.46154, –1.05517, –0.52139, –0.18486, 0.54573, 0.68696, 1.09425, 1.12874, 1.78430, 2.41943, 2.77533	–2.60318, –2.40073, –2.06165, –1.66599, –1.44707, –1.29173, –0.42388, 0.73233, 0.93137, 1.20248, 1.34510, 1.75222, 1.95559, 2.35711
C_{70}	K	–2.64515, –2.12435, –1.78737, –1.43566, –1.05474, –0.40545, –0.09433, 0.61803, 0.81185, 1.09426, 1.21902, 1.82482, 2.43544, 2.77968	–2.62463, –2.56054, –2.13642, –1.69070, –1.61745, –1.32018, –1.25467, 0.72228, 0.74990, 1.19940, 1.27053, 1.74743, 1.92797, 2.35103

Table 4. Eigenvalues of the graphs shown in Figs. 1-4 resulting from $b = \pm 1, -2$ for 6-fold symmetry

		Eigenvalues		
System	Graph	Doubly degenerate	Doubly degenerate	Non-degenerate
C_6	(A′)	1.00000	–1.00000	–2.06000
C_{l2}	(B′)	–0.61803, 1.61803	–1.61803, 0.61803	–2.41421, 0.41421
C_{24}	(C′)	–1.67513, –0.53918, 1.00000, 2.21431	–2.21431, –1.00000, 0.53918, 1.67513	–2.67513, –1.53918, 1.00000, 1.21431
C_{36}	(D′)	–2.08613, –1.41421 0.00000, 0.57199, 1.41421, 2.51413	–2.36846, –1.52615, –1.00000, 0.78771, 1.00000, 2.10709	–2.73205, –1.73205, –1.41421, 0.73205, 1.41421, 1.73205
C_{48}	(E′)	–2.38492, –1.63305, –0.91509, –0.24030, 0.74275, 1.00000, 1.77757, 2.65305	–2.43779, –1.88398, –1.19568, –1.00000, 0.60470, 1.23970, 1.37287, 2.30017	–2.74401, 1.84432, –1.73205, –1.24341, 0.90925, 1.00000, 1.73205, 1.92250

Table-4 (contd.)

C_{60}	(F′)	–2.55703, –1.80735, –1.35469, –0.76796, –0.18979, 0.64919, 0.90308, 1.31949, 2.07724, 2.72782	–2.48211, –2.08054, –1.41421, –1.26130, –0.92099, 0.69552, 0.92983, 1.41421, 1.71528, 2.40432	–2.74667, –1.93102, –1.90211, –1.48355, –1.17557, 0.79346, 1.17557, 1.34823, 1.90211, 2.01956
C_{72}	(G′)	–2.57837– –1.94851, –1.59932, –1.31787, –0.48203, –0.18479, 0.44232, 0.90287, 1.00000, 1.61074, 2.35166, 2.80330	–2.51919, –2.30082, –1.83747, –1.41421, –1.06197, –0.43848, 0.65308, 0.82092, 1.22800, 1.41421, 1.97560, 2.48033	–2.74667, –2.40479, –1.93102, –1.66278, –1.48355, –0.42305, 0.79346, 1.00000, 1.34823, –1.44457, 2.01956, –2.04605
C_{72}	(H′)	–2.57686, –1.92091, –1.54437, –1.30285, –0.30120, –0.14267, 0.72639, 0.90310, 1.22641, 1.72275. 2.39545, 2.81477	–2.53586, –2.35284, –1.90921, –1.41421, –1.16027, –0.94574, 0.56372, 0.76951, 1.14703, 1.41421, 1.94938, 2.4 7426	–2.74668, –2.74668, –1.93102, –1.93102, –1.48356, –1.48356, 0.79346, 0.79346, 1.34824, 1.34824, 2.01956, 2.01956
C_{72}	(I′)	–2.65843, –2.02505, –1.56219, –1.00000 –0.80367, –0.13642, 0.53851, 1.00000, 1.00000, 1.58896, 2.28528, 2.77301	–2.51417, –2.20086, –1.64055, –1.43883, –1.00000, –1.00000, 0.64784, 1.00000, 1.22064, 1.51119, 1.94749, 2.46724	–2.74728, –2.00000, –2.00000, –1.63254, –1.41421, –1.12344, 0.84700, 1.00000, 1.41421, 1.57965, 2.00000, 2.07661
C_{84}	(J′)	–2.67807, –2.09797, –1.75038, –1.45580, –1.00000, –0.53662, –0.11808, 0.45579, 0.73182, 1.00000, 1.26523, 1 .86794, 2.48364, 2.82473	–2.54816, –2.32477, –2.03219, –1.49124, –1.37755, –1.00000, –0.43366, 0.62435, 0.91966, 1.00000, 1.43972, 1.58148, 2.12406, 2.51829	–2.74816, –2.40497, –2.00000, –1.89089, –1.45439, –1.41421, –0.41870, 0.81467, 1.00000, 1.19066, 1.41421, 1.77532, 2.00000, 2.13646
C_{84}	(K′)	–2.67009, –2.08613, –1.70650, –1.41421, –1.00000, –0.39883, 0.00000, 0.57199, 1.00000, 1.00000, 1.41421, 1.94219, 2.51413, 2.83323	–2.56155, –2.36864, –2.08613, –1.52615, –1 .41421, –1. 00000, –1 .00000, 0.57199, 0.78771, 1.00000, 1.41421, 1.56155, 2.10709, 2.51413	–2.76155, –2.73205, –2.00000, –2.00000, –1.73205, –1.41421, –1.36332, 0.73205, 1.00000, 1.00000, 1.41421, 1.73205, 2.00000, 2.12488

in the '*bay*' regions of (F) and then five K_2 subgraphs vertically in the resulting *bays* of (I); joining the pendent vertices of J one gets the C_{70} fullerene structure (K). For this reason the series corresponding to the fullerene pairs (C_{60}, C_{70}) have five identical sub-structures. Variation of the total π-electron energy per atom in β unit for the structures and sub-structure of these two fullerenes having 5-fold rotational symmetry is displayed in Fig. 7(a); since β is negative, Fig. 7(a) reveals that the stability progressively increases with size of the sub-structures and a substantial increase is observed when the cage is closed. Similarly the pair of fullerenes C_{72} and C_{84} have six common sub-structures [(A′) to (F′)] and the final cage structures for both the fullerenes can be obtained from F′. Variation of total π-electron energy per atom

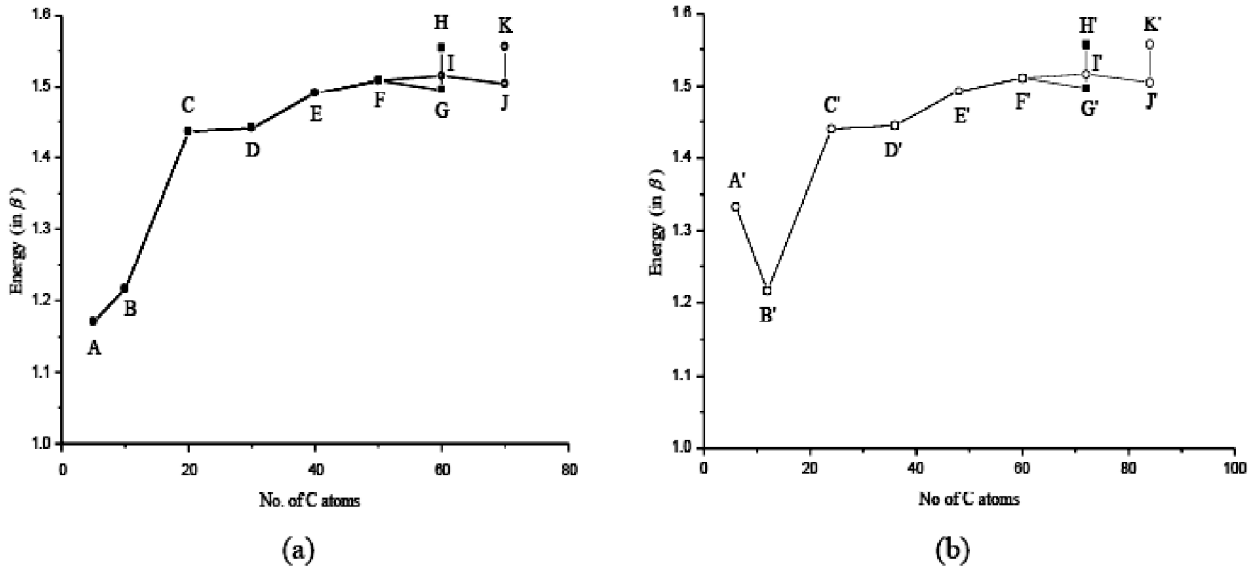

Fig. 7. Variation of total π-electron energy per atom in the series of sub-structures and structure of (a) C_{60} and C_{70} and (b) C_{72} and C_{84}.

Table 5. Total π-electron energy per atom for the structures and sub-structures

5-Fold rotational symmetry		6-Fold rotational symmetry	
Srtucture/ sub-structure	Total π-electron energy (in β) per atom	Srtucture/ sub-structure	Total π-electron energy (in β) per atom
A	1.17082	A′	1.33333
B	1.21601	B′	1.21676
C	1.43688	C′	1.44049
D	1.44121	D′	1.44508
E	1.49029	E′	1.49235
F	1.50848	F′	1.51076
G	1.49524	G′	1.49700
H	1.55302	H′	1.55650
I	1.51492	I′	1.51647
J	1.50390	J′	1.50480
K	1.55448	K′	1.55646

for this series is shown in Fig. 7(b). A steep decrease in stability from (A′) to (B′) (corresponding to benzene → 6-radialene) results from conversion of aromatic to non-aromatic structure; however, sharp increase in stability during cage closure [(G′) to (H′) for C_{72} and (J′) to (K′) for C_{84}] is observed in this series also.

7. Conclusion

By utilizing 5- and 6-fold rotational symmetries in conjunction with graph theoretical methods it has been established that the total π-electron energy per atom gradually decrease as the sub-structure grow in size with addition of C_2-fragments and in the last step when cage closure is complete, the stabilization is very much appreciable. This has been shown with four IPR fullerenes, namely, C_{60}, C_{70}, C_{72} and C_{84}.

References

1. R. Taylor, *J. Chem. Soc., Perkin Trans. 2*, 1993, 813.
2. J. Taylor, H. Guo and J. Wang, *Phys. Rev. B*, 2001, **63**, 245407.
3. M. Brandbyge, J. Mozos, P. Ordejon, J. Taylor and K. Stokbro, *Phys. Rev. B*, 2002, **65**, 165401.
4. Y. Xue, S. Datta and M. Ratner, *Chem. Phys.*, 2002, **281**, 151.
5. P. Damle, A. Ghosh and S. Datta, *Chem. Phys.*, 2002, **281**, 171.
6. F. Jiang, Y. Zhou, H. Chen, R. Note, H. Mizuseki and Y. Kawazoe, *Phys. Rev. B*, 2005, **72**, 155408.
7. J. R. Dias, "Molecular Orbital Calculations using Chemical Graph Theory", Springer-Verlag, Berlin, 1993.
8. N. Trinajstić, "Graph Theory and Molecular Orbitals in Chemical Graph Theory: Introduction and Fundamentals", eds. D. Bonchev and D. H. Rouvray, Gordon and Breach Science Publishers, New York, 1991, pp. 235-280.
9. D. C. Mukherjee, K. Datta and A. K. Mukherjee, *Indian J. Chem.*, 2001, **40A**, 126.
10. B. Mandal, M. Banerjee and A. K. Mukherjee, *Phys. Chem. Chem. Phys.*, 2004, **6**, 2040.
11. K. Datta, M. Banerjee and A. K. Mukherjee, *Phys. Chem. Chem. Phys.*, 1999, **1**, 2919.
12. B. C. Ghosh, *Indian J. Chem.*, 2019, **96**, 693.
13. R. A. Davidson, *Theor. Chim. Acta*, 1981, **58**, 193.
14. M. Shen, *Int. J. Quantum Chem.*, 1990, **38**, 551.